Electron Transfer in Acetohydroxy Acid Synthase as a Side Reaction of Catalysis. Implications for the Reactivity and Partitioning of the Carbanion/Enamine Form of (α-Hydroxyethyl)thiamin Diphosphate in a "Nonredox" Flavoenzyme†

Kai Tittmann,*,‡ Kathrin Schröder,‡ Ralph Golbik,‡ Jennifer McCourt,§ Alexander Kaplun,|| Ronald G. Duggleby,§ Ze'ev Barak,|| David M. Chipman,|| and Gerhard Hübner‡

Institut für Biochemie, Martin-Luther-Universität Halle-Wittenberg, Kurt-Mothes-Strasse 3, D-06099 Halle, Germany, Department of Biochemistry and Molecular Biology, The University of Queensland, Brisbane, Australia, and Department of Life Sciences, Ben-Gurion University of the Negev, Beer-Sheva, Israel

Received January 13, 2004; Revised Manuscript Received May 13, 2004

ABSTRACT: Acetohydroxy acid synthases (AHAS) are thiamin diphosphate- (ThDP-) and FAD-dependent enzymes that catalyze the first common step of branched-chain amino acid biosynthesis in plants, bacteria, and fungi. Although the flavin cofactor is not chemically involved in the physiological reaction of AHAS, it has been shown to be essential for the structural integrity and activity of the enzyme. Here, we report that the enzyme-bound FAD in AHAS is reduced in the course of catalysis in a side reaction. The reduction of the enzyme-bound flavin during turnover of different substrates under aerobic and anaerobic conditions was characterized by stopped-flow kinetics using the intrinsic FAD absorbance. Reduction of enzyme-bound FAD proceeds with a net rate constant of $k' = 0.2\ s^{-1}$ in the presence of oxygen and approximately $1\ s^{-1}$ under anaerobic conditions. No transient flavin radicals are detectable during the reduction process while time-resolved absorbance spectra are recorded. Reconstitution of the binary enzyme−FAD complex with the chemically synthesized intermediate 2-(hydroxyethyl)-ThDP also results in a reduction of the flavin. These data provide evidence for the first time that the key catalytic intermediate 2-(hydroxyethyl)-ThDP in the carbanionic/enamine form is not only subject to covalent addition of 2-keto acids and an oxygenase side reaction but also transfers electrons to the adjacent FAD in an intramolecular redox reaction yielding 2-acetyl-ThDP and reduced FAD. The detection of the electron transfer supports the idea of a common ancestor of acetohydroxy acid synthase and pyruvate oxidase, a homologous ThDP- and FAD-dependent enzyme that, in contrast to AHASs, catalyzes a reaction that relies on intercofactor electron transfer.

Acetohydroxy acid synthases (AHAS, EC 4.1.3.18) belong to the superfamily of enzymes using the cofactor ThDP[1] as the biologically active form of vitamin B_1. AHAS is a key enzyme in branched-chain amino acid metabolism in plants, fungi, bacteria, and archaea and catalyzes the condensation of pyruvate with either another pyruvate molecule or, alternatively, 2-ketobutyrate, yielding acetolactate or acetohydroxybutyrate as the precursors in valine, leucine, and isoleucine biosynthesis (reactions 1 and 2) (*1*). In addition

$$\text{pyruvate} + \text{pyruvate} \rightarrow \text{CO}_2 + \text{acetolactate} \rightarrow\rightarrow \text{valine, leucine} \quad (1)$$

$$\text{pyruvate} + \text{2-ketobutyrate} \rightarrow \text{CO}_2 + \text{acetohydroxybutyrate} \rightarrow\rightarrow \text{isoleucine} \quad (2)$$

to ThDP and Mg^{2+} that is required for anchoring the diphosphate moiety of ThDP, AHAS binds one molecule of flavin adenine dinucleotide (FAD) per active site in a noncovalent manner (*2*). Although the catalytic cycle involves no redox transformation of substrates to products, binding of FAD is mandatory for the catalytic activity of AHAS (*2*). The physiological condensation reaction is virtually unaffected by reduction of the enzyme-bound FAD or by substituion of FAD with the FAD analogues 8-chloro-FAD or 5-deaza-5-carba-FAD, thus ruling out a "hidden" or internal redox change (*3*). Aside from AHAS, only a few flavoenzymes are known that do not catalyze a net redox reaction despite an absolute requirement for FAD, as, for example, oxynitrilase (EC 4.1.2.10) or glyoxylate carboligase (EC 4.1.1.47) (*4*−*7*).

In the recently solved X-ray crystallographic structure of yeast AHAS (*Y*AHAS) the cofactors ThDP and FAD are

† This work was supported by the Fonds der chemischen Industrie (Halle), Grant 660/01 from the Israel Science Foundation (Beer-Sheva), and Grant A09937067 from the Australian Research Council (Brisbane).

* To whom correspondence should be addressed: e-mail, kai@bc.biochemtech.uni-halle.de; phone, ++49-345-5524887; fax, ++49-345-5527011.

‡ Martin-Luther-Universität Halle-Wittenberg.

§ The University of Queensland.

|| Ben-Gurion University of the Negev.

[1] Abbreviations: *Ec*AHAS, acetohydroxy acid synthase from *Escherichia coli*; *Y*AHAS, acetohydroxy acid synthase from yeast; *Lp*POX, pyruvate oxidase from *Lactobacillus plantarum*; *Ec*POX, pyruvate oxidase from *Escherichia coli*; ThDP, thiamin diphosphate; HEThDP, 2-(α-hydroxyethyl)thiamin diphosphate; $HEThDP^-$, carbanion/enamine form of HEThDP; AcThDP, 2-acetylthiamin diphosphate; LThDP, 2-lactylthiamin diphosphate; ALThDP, 2-(acetolactyl)thiamin diphosphate; AHBThDP, 2-(acetohydroxybutyryl)thiamin diphosphate; FAD, flavin adenine dinucleotide.

10.1021/bi049897t CCC: $27.50
Published on Web 06/18/2004

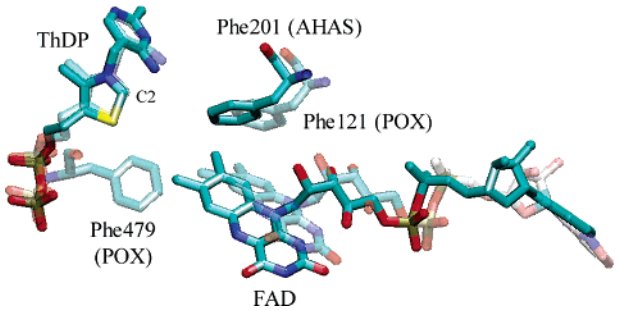

FIGURE 1: Superimposition of the cofactors FAD and ThDP and selected amino acid residues in the active sites of *Lp*POX (transparent) and *Y*AHAS (opaque) (*8*, *9*). Spatial coordinates of ThDP from both enzymes were superimposed with a least squares algorithm using the program VMD (*36*).

separated by approximately 6 Å (*8*). The spatial orientation and the distance between the two cofactors in AHAS are very similar to those in pyruvate oxidase from *Lactobacillus plantarum* (*Lp*POX, EC 1.2.3.3) as depicted in a superimposition of the active sites of the two enzymes (Figure 1) (*8*, *9*). Rather than promoting condensation of two keto acids, pyruvate oxidase catalyzes a fast intramolecular transfer of two electrons ($k \approx 400\ s^{-1}$) from the key catalytic intermediate (α-hydroxyethyl)-ThDP in the carbanion/enamine form ($HEThDP^-$) to the adjacent FAD, yielding 2-acetyl-ThDP (AcThDP) and fully reduced FAD (*10*, *11*). On the basis of the structural data two aromatic side chains (Phe 479, Phe 121) in the active site of *Lp*POX were suggested to participate in electron transfer as charge relays (*9*). One of these phenylalanines appears to be conserved in POX and AHAS and occupies similar positions in the two enzymes (Figure 1).

Recent kinetic studies on the steady-state distribution of covalent ThDP intermediates of bacterial AHAS isozyme II (Figure 2) showed that the addition of the first pyruvate to ThDP (step 2 in Figure 2, $k'_2 = 24\ s^{-1}$) resulting in the formation of 2-lactyl-ThDP (LThDP) is the rate-determining step of catalysis (*12*). The minor populations of the intermediates LThDP, $HEThDP^-$, and ALThDP under steady-state conditions imply low kinetic significance of the decarboxylation of LThDP (step 3, $k'_3 = 530\ s^{-1}$), the covalent addition of the second 2-keto acid to $HEThDP^-$ (step 4, $k'_4 = 1000\ s^{-1}$), and the product release (step 5, $k'_5 = 176\ s^{-1}$) with respect to the overall rate constant ($k_{cat} = 20\ s^{-1}$). In line with these results only ~0.01 mol of HEThDP/mol of enzyme was isolated using [^{14}C]pyruvate (*13*).

Aside from the physiological condensation reaction, an oxygenase side reaction has been observed that proceeds with about 1% of the rate of the synthase reaction (*14*, *15*). This oxygen-consuming reaction results in the formation of peracetic acid and is most likely due to the electrophilic attack of oxygen on the carbanionic form of HEThDP and the subsequent cleavage of the peracid (pathway II in Figure 3).

Here, we present experimental evidence that AHAS isozyme II from *Escherichia coli* catalyzes an intramolecular electron transfer reaction from $HEThDP^-$ to FAD (pathway III in Figure 3), resulting in the complete reduction of enzyme-bound FAD and the formation of AcThDP. The reductive and oxidative half-reactions of this side reaction of AHAS were kinetically characterized by pre-steady-state and steady-state kinetics using time-resolved spectroscopy. These results support the suggestion that AHAS enzymes could have been descended from pyruvate oxidase or a common ancestor (*16*). Although the absolute flavin requirement of AHAS appeared to be only a vestigial remnant of enzyme evolution, our studies demonstrate a hitherto unobserved chemical reactivity of FAD in AHAS.

MATERIALS AND METHODS

Chemicals and Reagents. Sodium pyruvate, sodium ketobutyrate, ThDP, FAD, β-D-glucose, and glucose oxidase were obtained from Sigma Aldrich. Imidazole and magnesium sulfate (heptahydrate) were purchased from Merck, and Ni−agarose superflow was supplied from Qiagene. Tris(hydroxymethyl)aminomethane was obtained from AppliChem. The ThDP adduct HEThDP was chemically synthesized according to ref *17*. All other chemicals and reagents were of analytical grade and were purchased from commercial sources. Quartz doubly distilled water was used throughout the experiments.

Expression and Protein Purification. The plasmid pRSET-GM encoding wild-type *Ec*AHAS II with an N-terminal hexahistidine fusion was obtained by inserting the *Bam*HI−*Eco*RI fragment containing the ilvGM genes from pET-GM (*18*) into plasmid pRSET-A (Invitrogen). Most of the coding region was then replaced by inserting the *Nsi*I−*Eco*RI fragment from pRGM (*19*). For expression of the genes of *Ec*AHAS II the pRSET-GM plasmid was used to tranform *E. coli* BL21(DE3) cells. Cells were grown in Luria broth medium containing 100 μg/mL ampicillin in a thermostated shaker (200 rpm) at 37 °C to an optical density of about 0.5 at 600 nm. IPTG was added to a final concentration of 0.5 mM. After 4 h of further growth (same conditions as described above) cells were harvested by centrifugation at 8000*g* for 20 min at 4 °C, quickly frozen in liquid nitrogen, and stored at −80 °C. About 10 g of cells was suspended in 50 mM Tris-HCl, pH 7.6, with 10 mM imidazole, 500 mM potassium chloride, and 10 μM FAD and disrupted in a French press at 1200 bar (Gaulin, APV Homogeniser GmbH, Lübeck, Germany). Cell debris was separated by centrifugation at 30000*g* for 2 h at 4 °C. Nucleic acids were precipitated by the addition of 0.1% (w/v) streptomycin sulfate for 30 min at 6 °C and discarded after centrifugation at 30000*g* for 30 min at 4 °C. The clear supernatant was applied to the Ni−agarose column (1.6 × 10 cm). Elution was performed using a linear imidazole gradient (0−100%) of 150 mL of 50 mM Tris-HCl, pH 7.6, containing 400 mM imidazole and 500 mM potassium chloride at 1 mL/min^{-1}. The homogeneous fractions were pooled and concentrated using Vivaspin 15 microconcentrators (Vivascience, Germany). To ensure full saturation of the enzyme with the flavin cofactor, 500 μM excess FAD was added to AHAS for 30 min at 8 °C. Prior to stopped-flow and ^{1}H NMR experiments unbound FAD was removed by gel filtration (HiTrap 5 × 5 mL, Amersham Biosciences) in 0.1 M potassium phosphate buffer, pH 7.6, at 1 mL/min^{-1}. Isozymes I and III were cloned into expression vectors as hexahistidine fusion proteins. The preparation of these plasmids will be described in full elsewhere (V. Vinogradov, in preparation). Proteins were purified as described for isozyme II (see above).

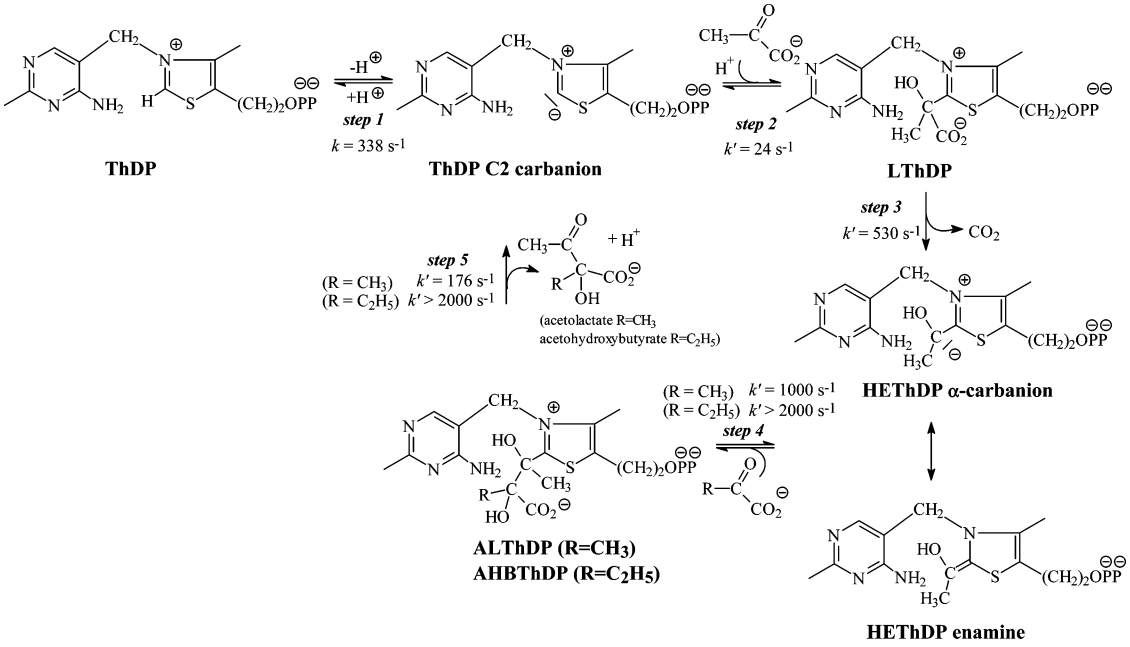

FIGURE 2: Catalytic cycle of AHAS with key intermediates and net rate constants of elementary steps according to refs *12* and *19*.

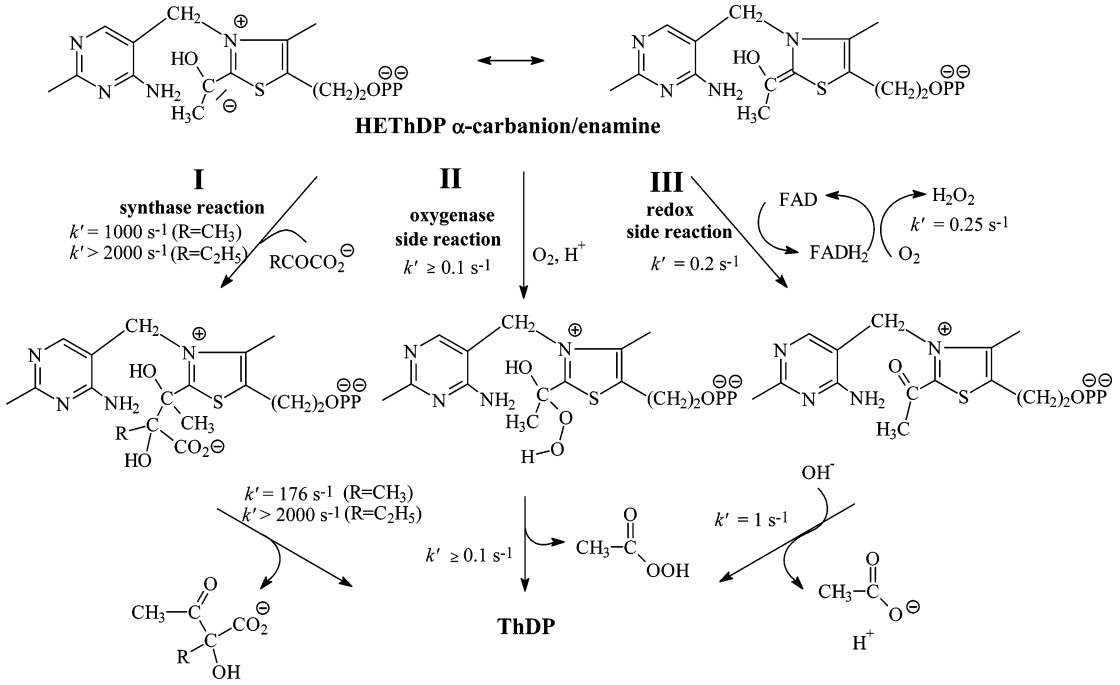

FIGURE 3: Partitioning of the catalytic key intermediate HEThDP (carbanion/enamine) in AHAS with net rate constants of elementary steps according to ref *12* and this study (see text).

The FAD-independent acetolactate synthase from *Klebsiella pneumoniae* was cloned, expressed, and purified as described elsewhere (*20*).

Determination of Protein Concentration. The purified protein was quantified by absorbance using an extinction of 0.9 A_{280nm} mg^{-1} mL cm^{-1} for the binary enzyme−FAD complex (*3*) and by the method of Bradford (*21*).

Activity Assays. The catalytic activity of AHAS was monitored spectrophotometrically following pyruvate consumption directly at 333 nm (ϵ = 17.5 M^{-1} cm^{-1}) or 350 nm (ϵ = 13.2 M^{-1} cm^{-1}) in 0.1 M potassium phosphate buffer, pH 7.6 at 37 °C (*3*), or according to ref *19*. In addition, enzyme-catalyzed substrate turnover and product formation were analyzed by ^{1}H NMR spectroscopy using the ^{1}H NMR signals of the methyl groups of pyruvate at 2.45 ppm (singlet, C**H**$_3$−CO−CO_2^-) and at 1.45 ppm [singlet, C**H**$_3$−C(OH)$_2$−CO_2^-, hydrated form] and of acetolactate at 2.26 ppm [singlet, CH_3−C(OH)−COC**H**$_3$−CO_2^-] and at 1.47 ppm [singlet, C**H**$_3$−C(OH)−$COCH_3$−CO_2^-]. One unit is defined as the amount of enzyme that catalyzes the formation of 1 μmol of acetolactate per minute from 2 μmol of pyruvate.

Stopped-Flow Kinetics. Rapid reaction experiments were carried out with an SX18 MV stopped-flow spectrometer (Applied Photophysics). The binary enzyme−FAD complex was preincubated with 1 mM ThDP and 5 mM Mg^{2+} for 5 min at 37 °C. Reconstituted holo-AHAS was mixed with varied concentrations of substrates (pyruvate, 2-ketobutyrate)

in 0.1 M potassium phosphate buffer, pH 7.6 at 37 °C. Anaerobic experiments were perfomed as described in ref *11*. Single-wavelength measurements were carried out at 451 nm and an optical path length of 10 mm. A total of 2000 data points were collected per experiment. Time-resolved absorbance spectra were recorded using a diode array detector (Applied Photophysics) and a 10 mm optical path length. The wavelength range was from 300 to 700 nm, and the acquisition time of the diode array detector was set at 2.56 ms per spectrum. Kinetic traces were fitted using the programs KaleidaGraph (Synergy Software) and Sigma Plot (Jandel Scientific) and appropriate algorithms.

Product Analysis. On the basis of differences in the chemical shifts of the methyl signals in the ^{1}H NMR spectra, both the products of the physiological condensation reaction (acetolactate and acetohydroxybutyrate) and of the hydrolytic/phosphorolytic cleavage of AcThDP (acetate and acetyl phosphate) can be quantitatively analyzed. The ^{1}H NMR methyl signals of acetolactate are two singlets at 1.47 and 2.26 ppm, and those of acetohydroxybutyrate are one singlet at 2.28 ppm (acetyl moiety) and a triplet at 0.83 ppm, respectively. Under the conditions used for NMR analysis (0.1 M potassium phosphate, pH 7.6 at 37 °C) acetyl phosphate (singlet at 2.14 ppm) undergoes no significant decomposition to acetate (singlet at 1.93 ppm) and phosphate.

RESULTS AND DISCUSSION

The ability of AHAS to transfer reducing equivalents to the flavin cofactor was initially observed when the holoenzyme was reacted with the substrates in a hermetically sealed NMR tube and in prolonged assays (~2 h) in normal cuvettes. In the course of substrate conversion (monitored by ^{1}H NMR or A_{333} measurements) bleaching of the yellowish solution was visible to the naked eye. Excess FAD, added to ensure full saturation of the enzyme, was also completely reduced. When the colorless solution was bubbled with air, it started to turn to yellow, reflecting flavin reoxidation.

It has been reported (*22*) that acetolactate is able to reduce FAD. Therefore, the observed bleaching might reflect the chemistry of the product rather than an intrinsic property of AHAS. To examine this hypothesis, the FAD-independent acetolactate synthase from *K. pneumoniae* was substituted for AHAS II in similar experiments with excess FAD. No FAD reduction was observed. Therefore, it can be concluded that the FAD bleaching is unrelated to the potential reduction of FAD by acetolactate. This result shows that FAD reduction is a side reaction catalyzed by AHAS and implies the involvement of bound FAD rather than the excess FAD in solution.

An inspection of the UV−vis absorbance spectra of AHAS II prior to (curve A in Figure 4) and after (curve B in Figure 4) complete substrate turnover revealed that the major part of the enzyme-bound flavin was converted to $FADH_2$. The intensity ratio of the two lowest $\pi \rightarrow \pi^*$ transitions at 378 and 451 nm of oxidized FAD in AHAS is slightly inverted with respect to free FAD, as already found for pyruvate oxidase from *L. plantarum* (*11*). No absorbance indicative of a flavin semiquinone could be observed in this type of experiment.

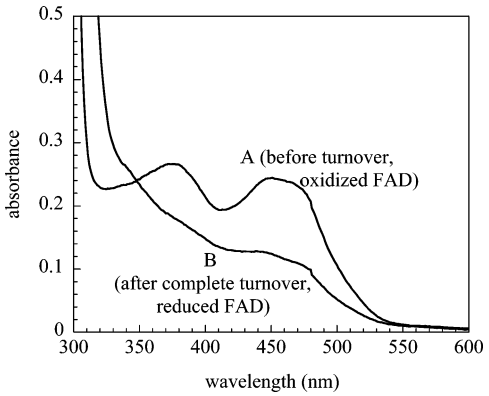

FIGURE 4: UV−vis absorbance spectra of *Ec*AHAS II prior to (A) and after (B) complete substrate turnover. *Ec*AHAS II (29 μM active site concentration) was incubated with 50 mM pyruvate, 1 mM ThDP, and 5 mM Mg^{2+} in 0.1 M potassium phosphate buffer, pH 7.6 at 37 °C, until complete pyruvate exhaustion. Spectra are corrected for buffer contributions.

To analyze the kinetics of FAD reduction in AHAS during substrate turnover, stopped-flow experiments were carried out under both aerobic and anaerobic conditions.

Course of FAD Reduction during AHAS Catalysis under Aerobic Conditions. Reduction of enzyme-bound FAD in AHAS during substrate turnover monitored at 451 nm consists of several phases (Figure 5). Initially, a decrease in absorbance can be observed. This pre-steady-state phase (k_{obs} = 0.45 s^{-1}) reflects the redox reaction of $HEThDP^-$ and FAD and all preceding steps in catalysis, such as the formation of LThDP and its decarboxylation (see Figure 2), and is followed by a short steady-state phase of the redox cycle where the apparent rate of FAD reduction by $HEThDP^-$ equals the rate of flavin reoxidation by oxygen. As dissolved oxygen is consumed, the ratio of $FAD/FADH_2$ is shifted to $FADH_2$ until complete reduction of the enzyme-bound FAD. The concentration ratio of oxidized and reduced FAD species in the steady state of the redox cycle (compare Figure 5) at substrate saturation is equal to the ratio of the net rate constants of the reductive (k'_{red}) and oxidative (k'_{ox}) half-reactions according to eq 3. Therefore, an estimate of the

$$\frac{[\mathrm{E{-}FAD}]}{[\mathrm{E{-}FADH_2}]} = \frac{k'_{ox}}{k'_{red}} \tag{3}$$

net rate constant of the oxidative half-reaction can be calculated as

$$k'_{ox} = \frac{A(451)_\infty - A(451)_{ss}}{A(451)_{ss} - A(451)_0} k'_{red} \tag{4}$$

where $A(451)_\infty$ represents the absorbance at 451 nm after complete reduction of the enzyme, $A(451)_{ss}$ the absorbance at steady state of the redox cycle, and $A(451)_0$ the absorbance prior to reaction of the enzyme with the substrate.

In terms of kinetics, the observed rate constant of the pre steady state reflects both the overall forward rate constant of the reductive half-reaction (k'_{red}) and that of the oxidative half-reaction (k'_{ox}) (eq 5). In analogy to reversible reactions, the sum of the rate constants of the forward and reverse reaction represents the observed rate constant.

$$k_{obs} = k'_{red} + k'_{ox} \tag{5}$$

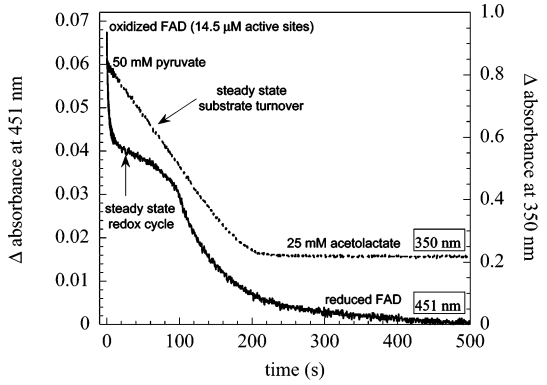

FIGURE 5: Progress curve of the reaction of *Ec*AHAS II with pyruvate monitored at 451 nm (intrinsic FAD absorbance) and 350 nm (pyruvate absorbance) under aerobic conditions. *Ec*AHAS II (14.5 μM active site concentration) was incubated with 50 mM pyruvate, 1 mM ThDP, and 5 mM Mg^{2+} in 0.1 M air-saturated potassium phosphate buffer, pH 7.6 at 37 °C. The optical path length was 10 mm, and a total of 2000 data points were collected. Kinetic traces were analyzed according to refs *23* and *3*.

As it concerns the reductive half-reaction, covalent binding of pyruvate to ThDP ($k'_2 = 24\ s^{-1}$) and decarboxylation of the thereby formed LThDP ($k'_3 = 530\ s^{-1}$) can be excluded as rate-determining steps. Therefore, the pre-steady-state phase can be attributed mainly to the reduction of FAD by $HEThDP^-$ and the reoxidation of the flavin by oxygen (eq 5) (*12*). Taking into account a steady-state concentration ratio of [E−FAD]/[E−$FADH_2$] of 1.3 (see Figure 5), a $k_{obs} = 0.45\ s^{-1}$ and, according to eq 5, a k'_{red} of 0.2 s^{-1} and a k'_{ox} of 0.25 s^{-1} can be estimated.

Simultaneous with the observation of the flavin absorbance during substrate turnover, pyruvate consumption was monitored directly at 350 nm ($\epsilon_{pyruvate} = 13.2\ M^{-1}\ cm^{-1}$). As depicted in Figure 5, pyruvate (50 mM) is steadily and completely converted to acetolactate, and neither a lag nor a burst phase can be observed. Evidently, flavin reduction and the concomitant oxygen consumption occur in the steady state of the catalytic cycle of the physiological synthase reaction. Analysis of the progress curves monitored at 451 nm according to the method of Gibson et al. (*23*) revealed a catalytic constant of the futile redox cycle (O_2 turnover) of approximately 0.1 s^{-1} (Table 1). When AHAS is reacted with pyruvate and 2-ketobutyrate (25 mM each), the oxygen consumption is significantly slower (0.019 s^{-1}) (Table 1). The amplitude of the pre-steady-state phase is very small (data not shown), which implies an altered ratio of the rates of the reductive and oxidative half-reactions. On the basis of the assumption that the rate of reoxidation of reduced FAD by oxygen is independent of the chemical nature of the substrates reacting at the ThDP site and a steady-state concentration ratio of [E−FAD]/[E−$FADH_2$] ≈ 7, the rate of the reductive half-reaction can be calculated to $k'_{red} = 0.035\ s^{-1}$ using eq 3 (Table 1).

To shift the partitioning of the $HEThDP^-$ intermediate in favor of the redox reaction, flavin reduction in AHAS was followed in the presence of very low substrate concentrations (2.5 mM), conditions under which the condensation reaction of $HEThDP^-$ and the second keto acid is slowed (assuming saturation for the first keto acid and nonsaturation for the second; see ref *2*). Oxygen consumption via the redox cycle (0.017 s^{-1}) is clearly slower under the conditions indicated in comparison to substrate saturation (0.095 s^{-1}) (Table 1). The rate of the pre-steady-state phase is slightly faster than at high substrate conditions (Table 1).

The results presented here provide convincing evidence that the cofactor FAD in AHAS is reduced in the course of substrate turnover as a result of the partitioning of $HEThDP^-$. Due to the fact that the progress curves of aerobic FAD reduction are of a typical flavin oxidase type and consist of a pre-steady-state, a steady-state, and an oxygen-consuming phase, it is reasonable to assume a futile redox cyle of the flavin cofactor involving reduction by $HEThDP^-$ and reoxidation by oxygen (pathway III in Figure 3).

$$\text{E}-\text{ThDP/FAD} + \text{pyruvate} \rightarrow \text{CO}_2 + \text{E}-\text{HEThDP}^-/\text{FAD} + \text{H}^+ \rightarrow \text{E}-\text{AcThDP/FADH}_2 \text{ (reductive half-reaction)} \quad (6)$$

$$\text{E}-\text{AcThDP/FADH}_2 + \text{O}_2 + \text{OH}^- \rightarrow \text{H}_2\text{O}_2 + \text{acetate} + \text{E}-\text{ThDP/FAD} \text{ (oxidative half-reaction)} \quad (7)$$

The specific activity of AHAS for oxygen turnover is about 0.5% of its physiological synthase reaction. It must be noted that oxygen consumption during AHAS catalysis cannot solely be attributed to the oxygenase side reaction (compare Figure 3) as proposed earlier (*14*, *15*). At substrate saturation at least a significant part of soluble oxygen is consumed via the redox cycle. The oxygenase side reaction may account for most of the O_2 consumption at low substrate concentrations (*15*). At saturation, the second keto acid very likely occludes the active site, preventing electrophilic attack of O_2 on $HEThDP^-$, and thereby favors both the condensation reaction and the competing intramolecular redox side reaction. As expected, both the redox reaction and the oxygenase reaction are slowed when AHAS is reacted with a mixture of pyruvate and 2-ketobutyrate, which is preferred 60-fold over pyruvate as an alternative second substrate (*1*).

Course of FAD Reduction during AHAS Catalysis under Anaerobic Conditions. As outlined in the previous section, partitioning of the $HEThDP^-$ intermediate is controlled by the reactivity and effective active site concentrations of the electrophiles pyruvate, 2-ketobutyrate, and oxygen. To suppress the oxygenase side reaction, turnover experiments were carried out under anaerobic conditions. Under these conditions, only partitioning between keto acid addition to $HEThDP^-$ and electron transfer from the latter to FAD is expected to occur. Moreover, reoxidation of reduced FAD by oxygen is prevented, thus allowing a kinetic analysis of the reductive half-reaction.

Reduction of FAD in AHAS monitored by flavin absorbance at 451 nm during substrate turnover under anaerobic conditions consists of several phases and is completed after 100 s (Figure 6). A kinetic analysis of the reduction process in the presence of either pyruvate as the sole substrate or a mixture of pyruvate and 2-ketobutyrate revealed the process to consist of at least three different phases that could be fitted using three single exponential terms (Figure 6, Table 2). Since we observe full time course kinetics, the assignment of three consecutive exponentials is phenomenological in the first instance and might not necessarily reflect the complexity of the reaction kinetics. As summarized in Table 2, the first phase accounting for reduction of the major part of FAD in

Table 1: Specific Activities and Catalytic Constants of the Physiological Synthase Reaction and the Futile Redox Cycle of *Ec*AHAS II and Net Rate Constants of the Reductive and Oxidative Half-Reactions of the Redox Cycle[a]

substrate concn	O_2 consumption via redox cycle[b] (μmol min^{-1} mg^{-1})	k_{cat} redox cycle (s^{-1})	activity of synthase reaction[c] (μmol min^{-1} mg^{-1})	k_{cat} synthase reaction (s^{-1})	concn ratio of [E−FAD]/[E−FADH$_2$] at steady state (redox cycle)	k'_{red} (s^{-1})	k'_{ox} (s^{-1})
50 mM pyruvate	0.084	0.095	17.5	20	1.3	0.20	0.25
25 mM pyruvate + 25 mM α-ketobutyrate	0.017	0.019	17.5	20	7.0	0.03	0.25
2.5 mM pyruvate	0.015	0.017	5	6	nd[d]	0.35	0.25

[a] See text. [b] According to the method of Gibson et al. (*23*), measured in 0.1 M potassium phosphate buffer, pH 7.6 at 37 °C, and considering a solubility of [O_2] = 0.21 mM at 37 °C. [c] According to ref *19* in 0.1 M potassium phosphate buffer, pH 7.6 at 37 °C. [d] Not determined since the concentration ratio of [E-FAD]/[E-FADH$_2$] can only be correlated to the rates of reductive and oxidative half-reactions at substrate saturation.

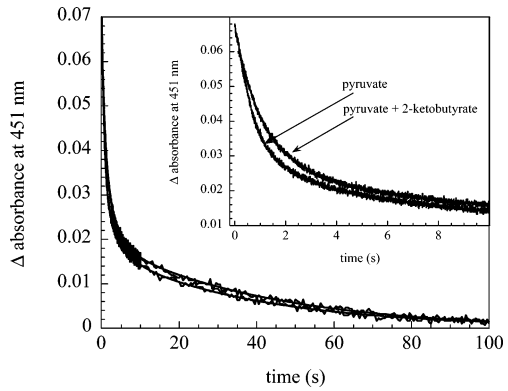

FIGURE 6: Progress curve of the reaction of *Ec*AHAS II with pyruvate monitored at 451 nm (intrinsic FAD absorbance) under anaerobic conditions. *Ec*AHAS II (14.5 μM active site concentration reconstituted with 1 mM ThDP and 5 mM Mg^{2+}) was incubated with either 50 mM pyruvate or 25 mM pyruvate and 25 mM 2-ketobutyrate in 0.1 M potassium phosphate buffer, pH 7.6 at 37 °C. Anaerobiosis was established as described in ref *11*. The optical path length was 10 mm, and a total of 2000 data points were collected. Kinetic traces were analyzed using a triple exponential function $y = y_0 + a_1 \exp(-k_1 t) + a_2 \exp(-k_2 t) + a_3 \exp(-k_3 t)$ with a_i representing the amplitudes and k_i the respective rate constants. Fitted curves are shown as solid lines (—), and the results are summarized in Table 2. Inset: Initial phase of the reaction.

AHAS is slightly faster than that observed under aerobic conditions. This is expected since competitive oxygenation of HEThDP$^-$ is excluded. The differences in the observed rates for FAD reduction in the presence of the alternative second substrates pyruvate and 2-ketobutyrate are only marginal (Table 2), even though 2-ketobutyrate is preferred 60-fold over pyruvate as the acceptor keto acid, and the forward rate constant of its covalent addition to HEThDP$^-$ ($k > 2000$ s^{-1}) was reported to be much larger than that observed for pyruvate ($k \approx 1000$ s^{-1}) (*12*). These findings point to a reversible noncovalent binding of the acceptor keto acid (KA) prior to its ligation to the carbanion/enamine of HEThDP, yielding the covalent acetohydroxy acid−ThDP adduct (E−AHAThDP):

$$\text{E}-\text{HEThDP}^- + \text{KA} \Leftrightarrow \text{E}-\text{HEThDP}^-*\text{KA (Michaelis complex)} \Leftrightarrow \text{E}-\text{AHAThDP} \quad (8)$$

Further evidence for a docking site of the acceptor substrate was presented by Schloss, who demonstrated that the competition between the acceptor substrate and oxygen saturates at less than 100% inhibition of the oxygenase side reaction (*15*).

A preliminary comparison of the reduction of enzyme-bound FAD in the three AHAS isozymes of *E. coli*, using purified enzymes under anaerobic conditions at saturating substrate concentration, indicates that the bound flavin is reduced at a similar overall rate in AHAS I and II (data not shown). The flavin bound to AHAS III is also reduced during turnover under these conditions, but the process is more than 1 order of magnitude slower. In contrast, we have observed no reduction of the bound FAD in glyoxylate carboligase during turnover in the presence of saturating amounts of its substrate glyoxylate as already described in ref *5*.

The multiple phases of anaerobic FAD reduction in AHAS II observed in Figure 6 either may be due to a stepwise electron transfer with transient formation of radical species or may be a result of the complexity of the partitioning of HEThDP$^-$. Apparently, a classic single turnover approach for the reductive half-reaction of AHAS cannot be applied under anaerobic conditions because of the competitive reactions of keto acid addition and electron transfer and the steady turnover of the substrate to the acetohydroxy acid, which itself is a substrate in the reverse reaction (*2*).

To test the possible intermediacy of radical species, time-resolved absorbance spectra of the enzyme-bound flavin were recorded during substrate turnover by AHAS II. The different spectroscopic properties of the oxidized, semireduced (radical), and fully reduced flavin allow an intermediate analysis of enzymatic redox reactions involving a flavin cofactor (*6*). In Figure 7, the time-resolved absorbance spectra of the enzyme-bound FAD during pyruvate turnover at substrate saturation (pyruvate = 50 mM) are depicted. The absorbance of the substrate pyruvate ($n \rightarrow \pi^*$ transition of the carbonyl function at 320 nm) interferes slightly with that of the flavin ($\pi \rightarrow \pi^*$ transitions at 378 and 451 nm), but, clearly, no absorbance indicative of a semireduced (radical) FAD can be observed (Figure 7, inset); rather, only the formation of fully reduced FAD is observable. Moreover, these data show that the reduction of FAD as a result of the partitioning of HEThDP$^-$ occurs in the steady state of the physiological catalytic cycle. Similar results were obtained for the reaction of AHAS with pyruvate and 2-ketobutyrate (data not shown). These observations have interesting kinetic implications for the electron transfer reaction. On the basis of the fact that the two cofactors are supposed to be separated by approximately 6 Å as in the homologous *Y*AHAS (*8*), neither a direct carbanion mechanism proceeding via a covalent ThDP−flavin adduct nor a hydride transfer seems to be likely unless the structure of AHAS II is strikingly different from yeast AHAS or there are large structural rearrangements during catalysis. Thus, the remaining likely pathway is a

Table 2: Forward Rate Constants of the Reductive Half-Reaction of *Ec*AHAS II under Anaerobic Conditions in the Presence of (a) 50 mM Pyruvate or (b) 25 mM Pyruvate and 25 mM 2-Ketobutyrate in 0.1 M Potassium Phosphate Buffer, pH 7.6, or (c) 50 mM Pyruvate in 0.1 M Potassium Phosphate Buffer (in D_2O), pD 7.6, or (d) 50 mM Pyruvate in 0.1 mM Potassium Phosphate Buffer, pH 6.0 at 37 °C[a]

	k_1 (s^{-1})	relative amplitude (%)	k_2 (s^{-1})	relative amplitude (%)	k_3 (s^{-1})	relative amplitude (%)
pyruvate + pyruvate (a)	1.27 ± 0.01	60 ± 1	0.22 ± 0.01	20 ± 2	0.026 ± 0.001	20 ± 2
pyruvate + 2-ketobutyrate (b)	1.06 ± 0.02	55 ± 1	0.28 ± 0.01	22 ± 2	0.023 ± 0.001	23 ± 2
pyruvate + pyruvate (D_2O) (c)	0.69 ± 0.02	50 ± 1	0.21 ± 0.01	28 ± 2	0.018 ± 0.001	22 ± 2
pyruvate + pyruvate (pH 6.0) (d)	3.71 ± 0.03	15 ± 2	0.32 ± 0.01	43 ± 1	0.027 ± 0.001	42 ± 1

[a] Progress curves of FAD reduction (compare Figure 6) were analyzed using a triple exponential function $y = y_0 + a_1 \exp(-k_1 t) + a_2 \exp(-k_2 t) + a_3 \exp(-k_3 t)$ with a_i representing the amplitudes and k_i the respective rate constants.

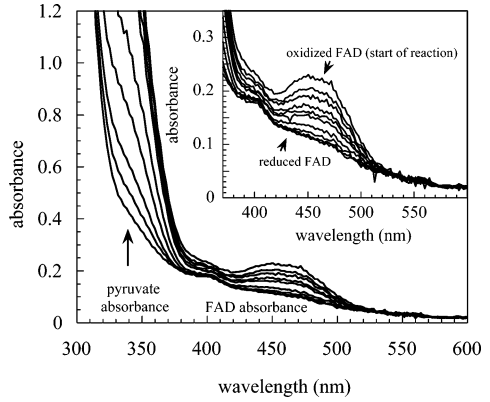

FIGURE 7: Time-resolved absorbance spectra of AHAS-bound FAD in the course of anaerobic substrate turnover. *Ec*AHAS II (29 μM active site concentration reconstituted with 1 mM ThDP and 5 mM Mg^{2+}) was incubated with 100 mM pyruvate in 0.1 M potassium phosphate buffer, pH 7.6 at 37 °C, under anaerobic conditions. Anaerobiosis was established as described in ref *11*. The optical path length was 10 mm. Spectra were recorded at 0.32, 2, 5.2, 15, 25, 50, 75, 100, 125, and 150 s after mixing. All spectra are corrected for buffer contributions. Inset: Zoomed section of flavin absorbance.

stepwise transfer of the electrons. The nonobservance of radical intermediates pinpoints the ratio of the rates of the two microscopic transfer steps: the transfer of the first reducing equivalent must be rate-limiting for the overall transfer. It remains unclear whether the apparent rate constants of the reductive half-reaction represent true or gated electron transfer events (*24*). These results concur with studies on the electron transfer reaction in pyruvate oxidase. Although only a very small kinetic solvent isotope effect has been determined for the reductive half-reaction and no reduction of the flavin analogue 5-deaza-5-carba-FAD was observed, thus ruling out a hydride transfer from $HEThDP^-$ to FAD, no radicals were detectable while time-resolved absorbance spectra were recorded (*11*, *25*, *26*). For AHAS, a somewhat larger kinetic solvent isotope effect of $k_H/k_D = 1.84$ can be observed for the fast phase of the reductive half-reaction (see Table 1), but on the basis of the arguments discussed above and the intercofactor distance of approximately 6 Å, this primary isotope effect rather reflects a proton than a hydride transfer.

Interestingly, at pH 6.0, well below the optimum for AHAS but close to that of pyruvate oxidase, the apparent rate of FAD reduction is increased (Table 2). This may be the consequence of an altered partitioning of the HEThDP enamine/carbanion in terms of a slowed ligation or a larger driving force of the redox reaction, but even at this pH the rate is 100-fold slower than that observed in pyruvate oxidase (*10*, *11*). At pH 7.6 both the acceptor substrate ligation ($k'_4 \approx 1000\ s^{-1}$) and product release ($k'_5 = 200\ s^{-1}$) have been shown not to be rate-limiting for the overall reaction ($k_{cat} = 20\ s^{-1}$) (*12*). The rather unusual pH optimum of the FAD-independent acetolactate synthases, also named "pH 6 acetolactate-forming enzymes", invites speculation that the FAD-dependent AHAS evolved at higher pH to specifically promote the synthase reaction and suppress the redox side reaction. In accord with this, the redox reaction of $HEThDP^-$ and FAD in pyruvate oxidase is significantly slower at pH 7.6 than at pH 6.0 (K. Tittmann, unpublished results).

FAD Reduction after Reconstitution of the Binary Apo−FAD Complex with HEThDP. Although substantial evidence has been accumulated that FAD in AHAS is reduced by the reaction intermediate HEThDP in its carbanion/enamine form, the ultimate proof for this chemical pathway would be the reduction of the flavin after reconstitution of the binary apo−FAD complex with chemically synthesized HEThDP under anaerobic conditions. In the absence of the acceptor substrates and oxygen neither the physiological ligation reaction nor the oxygenase side reaction can occur. However, some restrictions apply to the system. First, the binary enzyme−FAD complex must exhibit sufficient affinity toward HEThDP. Given this, the enzyme still has to ionize HEThDP (eq 9). As shown in model studies, only the carbanion/enamine form of HEThDP is redox active but not its protonated conjugated acid (*27*).

$$\text{apo}-\text{FAD} + \text{HEThDP} \Leftrightarrow \text{holo}-\text{FAD}-\text{HEThDP} \Leftrightarrow H^+ + \text{holo}-\text{FAD}-\text{HEThDP}^- \text{ (carbanion/enamine)} \quad (9)$$

$$\text{holo}-\text{FAD}-\text{HEThDP}^- \text{ (carbanion/enamine)} + H^+ \rightarrow \text{holo}-\text{FADH}_2-\text{AcThDP} \quad (10)$$

In Figure 8, a typical progress curve of FAD reduction after mixing apo−FAD enzyme with HEThDP and 1 mM Mg^{2+} is depicted. Clearly, part of the enzyme-bound FAD is reduced. Fitting the data revealed the process to consist of at least two single exponential phases with rate constants of $k_1 = 0.28 \pm 0.01\ s^{-1}$ (40% amplitude) and $k_2 = 0.049 \pm 0.001\ s^{-1}$ (60% amplitude). The rate of FAD reduction is smaller than that observed during substrate turnover (see Table 2), but as outlined above reversible binding and ionization may gate the redox reaction. Besides the verification of the intramolecular redox reaction, these data demonstrate that the enzymatic environment leads to tremendous stabilization of the zwitterionic form of HEThDP: model studies suggested a pK_a of approximately 18 for the ionization of HEThDP to the carbanion/enamine in the nonenzymatic system (*28*).

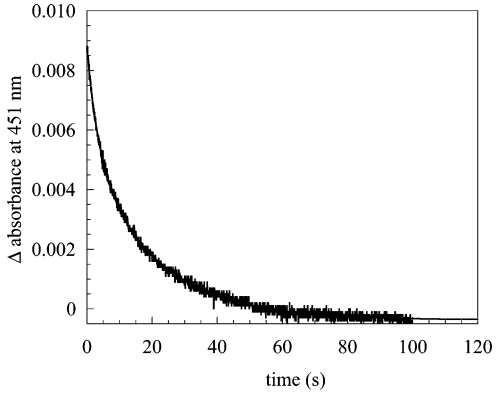

FIGURE 8: Progress curve of the reaction of *Ec*AHAS II with chemically synthesized HEThDP monitored at 451 nm (intrinsic FAD absorbance) under anaerobic conditions. The binary apo−FAD complex (14.5 μM active site concentration) was incubated with 1 mg/mL HEThDP and 5 mM Mg^{2+} in 0.1 M potassium phosphate buffer, pH 7.6 at 37 °C, under anaerobic conditions. Anaerobiosis was established as described in ref *11*. Kinetic traces were analyzed using a double exponential function $y = y_0 + a_1 \exp(-k_1 t) + a_2 \exp(-k_2 t)$ with a_i representing the amplitudes and k_i the respective rate constants. The fitted curve is shown as a solid line (—) and yielded rate constants of $k_1 = 0.28 \pm 0.01$ s^{-1} (40% amplitude) and $k_2 = 0.049 \pm 0.001$ s^{-1} (60% amplitude).

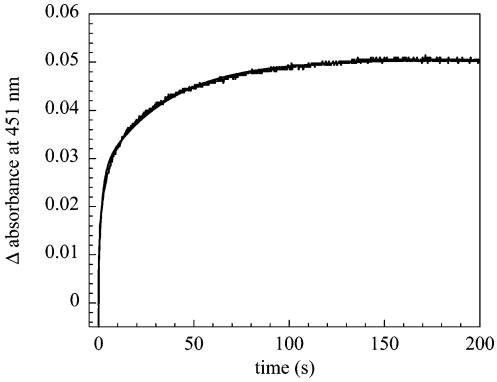

FIGURE 9: Progress curve of the reaction of reduced *Ec*AHAS II with oxygen monitored at 451 nm (intrinsic FAD absorbance). Holoenzyme (36 μM active site concentration) was incubated with 50 mM pyruvate in 0.1 M potassium phosphate buffer, pH 7.6 at 37 °C, under aerobic conditions until complete substrate turnover (compare Figure 5). Thereafter, the reduced enzyme was reacted with air-saturated buffer in a 1 + 1 mixing ratio at 37 °C. The optical path length was 10 mm, and a total of 2000 data points were collected. Kinetic traces were analyzed using a triple exponential function $y = y_0 + a_1[1 - \exp(-k_1 t)] + a_2[1 - \exp(-k_2 t)] + a_3[1 - \exp(-k_3 t)]$ with a_i representing the amplitudes and k_i the respective rate constants. The fitted curve is shown as a solid line (—) and yielded rate constants of $k_1 = 7.9 \pm 0.3$ s^{-1}, $k_2 = 0.49 \pm 0.01$ s^{-1}, and $k_3 = 0.028 \pm 0.001$ s^{-1}.

Reoxidation of Reduced $FADH_2$ in AHAS by Oxygen. The kinetic analysis of FAD reduction under aerobic conditions suggested a futile redox cycle comprising reduction by HEThDP$^-$ and reoxidation by oxygen. For a further kinetic characterization of the oxidative half-reaction, AHAS was reacted with pyruvate until full reduction of the enzyme and complete consumption of pyruvate and oxygen in the system. The reduced enzyme was then mixed with air-saturated buffer, and single wavelength progress curves as well as time-resolved spectra were recorded (Figures 9 and 10).

As observed above for the reductive half-reaction, the oxidative half-reaction consists of several phases. Fitting the progress curves suggested a minimum of three consecutive

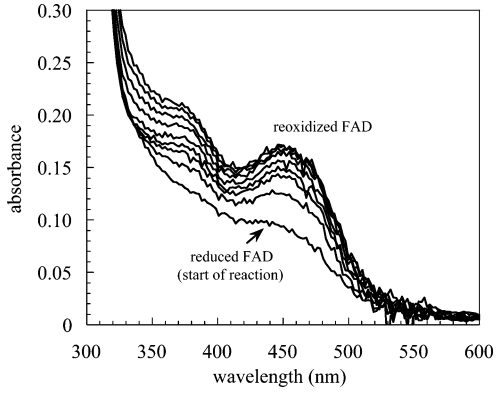

FIGURE 10: Time-resolved absorbance spectra of AHAS-bound FAD in the course of the oxidative half-reaction. Holoenzyme (43.5 μM active site concentration) was incubated with 50 mM pyruvate in 0.1 M potassium phosphate buffer, pH 7.6 at 37 °C, under aerobic conditions until complete substrate turnover (compare Figure 4). Thereafter, the reduced enzyme was reacted with air-saturated buffer in a 1 + 1 mixing ratio at 37 °C. The optical path length was 10 mm. Spectra were recorded at 0.32, 2, 5.2, 10, 20, 45, 70, 100, and 130 s after mixing. All spectra are corrected for buffer contributions.

(pseudo) first-order reactions with rate constants of $k_1 = 7.9 \pm 0.3$ s^{-1} (15% amplitude), $k_2 = 0.49 \pm 0.01$ s^{-1} (40% amplitude), and $k_3 = 0.028 \pm 0.001$ s^{-1} (45% amplitude). Since the rate constant of reoxidation of free reduced FAD was found to be $k_{obs} = 7.1 \pm 0.2$ s^{-1} (data not shown) under the same conditions (100 mM potassium phosphate, pH 7.6, 105 μM O_2, 37 °C), similar to the fast phase of AHAS reoxidation, it is reasonable to assume that part of the reduced FAD is released from the enzyme. While time-resolved spectra were recorded, no transient radical FAD species or flavin−oxygen adducts could be detected in the course of the oxidative half-reaction (Figure 10).

In view of the slow oxidation of reduced FAD by oxygen, the close relationship of AHAS to the class of membrane-associated pyruvate oxidases is highlighted. This type of pyruvate oxidases, such as from *E. coli*, acts as a direct electron shuttle to the respiratory chain: the reduced FAD in *Ec*POX is very unreactive toward oxygen but rather transfers the electrons to the mobile, membrane-soluble electron carrier ubiquinone 8 (*29*). In contrast, pyruvate oxidases from *Lactobacillae* catalyze the formation of the high-energy metabolite acetyl phosphate and rapidly reoxidize the reduced flavin by oxygen (*11*).

Product Analysis by ^{1}H NMR Spectroscopy and Implications for Partitioning of HEThDP$^-$. Using the different chemical shifts of the methyl signals of the product of the physiological synthase reaction acetolactate and that of the side redox reaction acetate, about 1.5% acetate with respect to acetolactate could be detected, corresponding to a $k_{cat} = 20$ s^{-1} (physiological reaction) and a $k_{cat} = 0.3$ s^{-1} (acetate formation) per active site. Acetyl phosphate cannot be detected as a reaction product. A comparison with the overall activity of oxygen turnover ($k_{cat} = 0.1$ s^{-1}; see Table 1) and the net rate constant of the redox reaction ($k' = 0.2$ s^{-1}; see Table 1) has interesting kinetic implications. First and foremost, it is obvious that the oxygen-consuming redox cycle does not account quantitatively for the observed acetate formation. Since peracetic acid, the product of the oxygenase side reaction (see Figure 3), was demonstrated to react rapidly with pyruvate, leading to the formation of two molecules of

acetate ($k = 20\ M^{-1}\ s^{-1}$) (*30*), the turnover number of the oxygenase side reaction can be estimated to $k = 0.1\ s^{-1}$ according to the equation:

$$v\ (\text{acetate oxygenase reaction}) = {}^{1}/_{2}[v\ (\text{acetate total}) - v\ (\text{acetate redox cycle})] \quad (11)$$

Another important conclusion can be drawn from the discrepancy between the net rate constant of the redox reaction ($k' = 0.2\ s^{-1}$) and the turnover number of the redox cyle ($k_{cat} = 0.1\ s^{-1}$). This implies that the redox reaction itself is not totally rate-determining for the redox cycle. Formation of LThDP ($k'_2 = 24\ s^{-1}$), decarboxylation of this intermediate ($k'_3 = 530\ s^{-1}$), and reoxidation of $FADH_2$ ($k'_{ox} = 0.25\ s^{-1}$) can be excluded as rate-determining events (*12*). Therefore, we suggest that hydrolysis of AcThDP might be at least partially rate-limiting for the futile redox cycle (Figure 3). At substrate saturation, k_{cat} (redox cycle) is defined as a function of rate constants of the individual steps k'_2 (formation of LThDP), k'_3 (decarboxylation of LThDP), k'_4 (redox reaction), k'_5 (hydrolysis of AcThDP), and k'_6 (k'_{ox}, reoxidation of $FADH_2$ by O_2) as follows:

$$\frac{1}{k_{cat}} = \frac{1}{k'_2} + \frac{1}{k'_3} + \frac{1}{k'_4} + \frac{1}{k'_5} + \frac{1}{k'_6} \quad (12)$$

$$k_{cat} = k'_2k'_3k'_4k'_5k'_6/(k'_2k'_3k'_4k'_5 + k'_2k'_3k'_4k'_6 + k'_3k'_4k'_5k'_6 + k'_2k'_4k'_5k'_6 + k'_2k'_3k'_5k'_6) \quad (13)$$

Using eqs 12 and 13, k_{cat} (redox cycle), and the previously determined rate constants k'_2, k'_3, k'_4, and k'_6 (k'_{ox}; see above), a forward rate constant of $k'_5 = 1.04\ s^{-1}$ can be estimated for the hydrolysis of AcThDP. Under comparable pH conditions but at lower temperature (pH 7.5, 24 °C) free acetyl-ThDP undergoes hydrolytic cleavage with a rate constant of $1\ s^{-1}$ (*31*), indicating that no mechanism other than solvent-mediated hydrolysis accounts for the release of acetate in AHAS.

In summary, partitioning of $HEThDP^-$ (Figure 3) is not reflected quantitatively in the ratio of the different products. Whereas formation of LThDP was found to be the rate-determining step for the physiological reaction of AHAS (*12*), the redox reaction of $HEThDP^-$ and FAD is rate-determining for the redox cycle. In addition, reversible binding of the reaction product acetolactate and cleavage of the thereby formed acetohydroxy acid−ThDP adduct to $HEThDP^-$ and pyruvate have to be taken into account (*2*).

CONCLUSIONS

The partitioning of the catalytic key intermediate $HEThDP^-$ in AHAS has been analyzed by a chemical quench/NMR technique (*12*), stopped-flow kinetics of FAD reduction, and product analysis (this work). Our studies show that the ligation of the acceptor keto acid to the carbanion/enamine form of HEThDP is a highly efficient process with forward rate constants of $k = 1000\ s^{-1}$ (acceptor pyruvate) and $k > 2000\ s^{-1}$ (acceptor ketobutyrate). A structural comparison of the active site geometry of AHAS and POX shows that both cofactors adopt similar positions (Figure 1). This is surprising since AHAS condenses two keto acids to the respective acetohydroxy acids and POX transfers two electrons from $HEThDP^-$ to the adjacent flavin. It is therefore of great interest to understand how the enzymes specifically promote either the condensation or redox reaction. Our studies here demonstrate for the first time that AHAS catalyzes an electron transfer between $HEThDP^-$ and FAD as a side reaction of catalysis. We were able to analyze kinetically the redox reaction using the intrinsic absorbance of the isoalloxazine of the flavin. Under anaerobic conditions the rate constant of FAD reduction is about $1\ s^{-1}$. In view of the overall catalytic activity ($k_{cat} = 20\ s^{-1}$), this is a rather fast side reaction. However, the extremely fast ligation reaction (see above) favors the partitioning to the physiological reaction and disfavors the nonproductive redox reaction. The closely related pyruvate oxidases sharing the same cofactor subset (ThDP, FAD) catalyze a fast electron transfer with rate constants in the range of $400\ s^{-1}$ (*10*, *11*). Two phenylalanines were suggested to participate in the electron transfer reaction, one of which is apparently conserved in AHAS and POX (Figure 1). This invites speculation about a specific role of the nonconserved phenylalanine (F479 in POX). Indeed, studies in our laboratory suggest to assign a specific role of this residue in the electron transfer reaction in *Lp*POX (G. Wille, G. Hübner, and K. Tittmann, in preparation). The apparent lack of electron transfer to FAD in *E. coli* glyoxylate carboligase, which has significant sequence similarity to the catalytic subunit of AHAS II, may be due to subtle differences in the conformation of the active sites of these enzymes or to a higher redox potential of the putative hydroxymethyl-ThDP anion/enamine intermediate.

No transient flavin radicals could be observed by time-resolved spectroscopy in the course of flavin reduction in AHAS. However, the large intercofactor distance and non-stacking of the thiazolium and isoalloxazine ring clearly favor a stepwise transfer of the electrons over a hydride transfer (*11*, *32*). Among the family of ThDP-dependent enzymes only pyruvate:ferredoxin oxidoreductase has been shown to transiently form detectable amounts of radical oxyethyl-ThDP species upon oxidation of the HEThDP enamine (*33*). No radicals could be detected in the course of the reductive half-reaction of *Lp*POX (*11*). The absence of a kinetic solvent isotope effect and the failure to reduce the flavin analogue 5-deaza-5-carba-FAD (a good hydride acceptor), however, suggest the transfer to occur rather stepwise than as a hydride (*11*).

The reduced flavin in AHAS is very unreactive toward oxygen, and in this way it very much resembles the pyruvate oxidase from *E. coli*, a membrane-associated enzyme that shuttles two electrons to the respiratory chain. It is noteworthy that *Ec*POX is activated by lipid binding, in contrast to the permanently activated POX from *Lactobacillae*. A single-step analysis revealed that electron transfer is stimulated from about $2\ s^{-1}$ to approximately $400\ s^{-1}$ by activation (*10*). The rate constant of electron transfer of nonactivated *Ec*POX is well in the range of that of *Ec*AHAS ($k \approx 1\ s^{-1}$). The nearly identical reactivities of nonactivated *Ec*POX and *Ec*AHAS in both the reductive and the oxidative half-reaction strongly support the hypothesis of a common ancestor of POX and AHAS (*16*). It is still an open question how the different enzymes evolved to favor a specific chemical path and avoid or at least disfavor undesired partitioning of the key intermediate $HEThDP^-$. Recently, we found evidence

that a conserved arginine, methionine, and tryptophan contribute to the specificity for ketobutyrate as the acceptor substrate in AHAS and are crucial for acceptor ligation (*34*, *35*, and submitted for publication). As a result, different partitioning of $HEThDP^-$ could be observed for the respective enzyme variants. We now hope to obtain further insights into the molecular origin of the divergent chemical fate of $HEThDP^-$ in AHAS and POX by comparative analyses of the partitioning of $HEThDP^-$ in active site variants (as well as in other AHAS isozymes and glyoxylate carboligase, which differ in their catalytic behavior from AHAS II) using the recently developed NMR/quench method (*12*) and the stopped-flow kinetics of FAD reduction as presented in this study.

ACKNOWLEDGMENT

We thank Sandro Ghisla for helpful discussions.

REFERENCES

1. Chipman, D. M., Barak, Z., and Schloss, J. V. (1998) Biosynthesis of 2-aceto-2-hydroxy acids: acetolactate synthases and acetohydroxyacid synthases, *Biochim. Biophys. Acta 1385*, 401−419.
2. Schloss, J. V., Van Dyk, D. E., Vasta, J. F., and Kutny, R. M. (1985) Purification and properties of *Salmonella typhimurium* acetolactate synthase isozyme II from *Escherichia coli* HB101/pDU9, *Biochemistry 24*, 4952−4959.
3. Schloss, J. V., and Van Dyk, D. E. (1988) Acetolactate synthase isozyme II from *Salmonella typhimurium*, *Methods Enzymol. 166*, 445−454.
4. Jorns, M. S. (1979) Mechanism of catalysis by the flavoenzyme oxynitrilase, *J. Biol. Chem. 254*, 12145−12152.
5. Chung, S. T., Tan, R. T., and Suzuki, I. (1971) Glyoxylate carboligase of *Pseudomonas oxalaticus*. A possible structural role for flavine-adenine dinucleotide, *Biochemistry 10*, 1205−1209.
6. Palfey, B. A., and Massey, V. (1998) Flavin-dependent enzymes, in *Comprehensive Biological Catalysis* (Sinnot, M., Ed.) Vol. 3, pp 83−154, Academic Press, London.
7. Bornemann, S. (2002) Flavoenzymes that catalyse reactions with no net redox change, *Nat. Prod. Rep. 19*, 761−772.
8. Pang, S. S., Guddat, L. W., and Duggleby, R. G. (2003) Molecular basis of sulfonylurea herbicide inhibition of acetohydroxyacid synthase, *J. Biol. Chem. 278*, 7639−7644.
9. Muller, Y. A., and Schulz, G. E. (1993) Structure of the thiamine- and flavin-dependent enzyme pyruvate oxidase, *Science 259*, 965−967.
10. Bertagnolli, B. L., and Hager, L. P. (1991) Activation of *Escherichia coli* pyruvate oxidase enhances the oxidation of hydroxyethylthiamin pyrophosphate, *J. Biol. Chem. 266*, 10168−10173.
11. Tittmann, K., Golbik, R., Ghisla, S., and Hübner, G. (2000) Mechanism of elementary catalytic steps of pyruvate oxidase from *Lactobacillus plantarum*, *Biochemistry 39*, 10747−10754.
12. Tittmann, K., Golbik, R., Uhlemann, K., Khailova, L., Schneider, G., Patel, M., Jordan, F., Chipman, D. M., Duggleby, R. G., and Hübner, G. (2003) NMR analysis of covalent intermediates in thiamin diphosphate enzymes, *Biochemistry 42*, 7885−7891.
13. Ciskanik, L. M., and Schloss, J. V. (1985) Reaction intermediates of the acetolactate synthase reaction: Effect of sulfometuron methyl, *Biochemistry 24*, 3357.
14. Abell, L. M., and Schloss, J. V. (1991) Oxygenase side reactions of acetolactate synthase and other carbanion-forming enzymes, *Biochemistry 30*, 7883−7887.
15. Tse, J. M. T., and Schloss, J. V. (1993) The oxygenase reaction of acetolactate synthase, *Biochemistry 32*, 10398−10403.
16. Chang, Y.-Y., and Cronan, J. E., Jr. (1988) Common ancestry of *Escherichia coli* pyruvate oxidase and the acetohydroxy acid synthases of the branched-chain amino acid biosynthetic pathway, *J. Bacteriol. 170*, 3937−3945.
17. Krampitz, L., Greull, G., Miller, C. S., Bicking, J. B., Skeggs, H. R., and Sprague, J. M. (1958) An active acetaldehyde-thiamin intermediate, *J. Am. Chem. Soc. 80*, 5893−5894.
18. Hill, C. M., Pang, S. S., and Duggleby, R. G. (1997) Purification of *Escherichia coli* acetohydroxyacid synthase isoenzyme II and reconstitution of active enzyme from its individual pure subunits, *Biochem. J. 327*, 891−898.
19. Bar-Ilan, A., Balan, V., Tittmann, K., Golbik, R., Vyazmensky, M., Hübner, G., Barak, Z., and Chipman, D. M. (2001) Binding and activation of thiamin diphosphate in acetohydroxyacid synthase, *Biochemistry 40*, 11946−11954.
20. Pang, S. S., Duggleby, R. G., Schowen, R. L., and Guddat, L. W. (2004) The crystal structures of Klebsiella pneumoniae acetolactate synthase with enzyme-bound cofactor and with an unusual intermediate, *J. Biol. Chem. 279*, 2242−2253.
21. Bradford, M. M. (1976) A rapid and sensitive method for the quantitation of microgram quantities of protein utilizing the principle of protein-dye binding, *Anal. Biochem. 72*, 248−254.
22. Park, H. S., Xing, R., and Whitman W. B. (1995) Nonenzymatic acetolactate oxidation to diacetyl by flavin, nicotinamide and quinone coenzymes, *Biochim. Biophys. Acta 1245*, 366−370.
23. Gibson, Q. H., Swoboda, B. E., and Massey, V. (1964) Kinetics and mechanism of action of glucose oxidase, *J. Biol. Chem. 239*, 3927−3934.
24. Davidson, V. L. (2002) Chemically gated electron transfer. A means of accelerating and regulating rates of biological electron transfer, *Biochemistry 41*, 14633−14636.
25. Tittmann, K., Proske, D., Spinka, M., Ghisla, S., Rudolph, R., Hübner, G., and Kern, G. (1998) Activation of thiamin diphosphate and FAD in the phosphate-dependent pyruvate oxidase from Lactobacillus plantarum, *J. Biol. Chem. 273*, 12929−12934.
26. Tittmann, K. (2000) Thesis, Martin-Luther-Universität Halle-Wittenberg.
27. Chiu, C. C., Pan, K., and Jordan, F. (1995) Modeling an elementary step of the enzyme pyruvate oxidase: Oxidation of a thiamin diphosphate-bound enamine intermediate by a flavin analog, *J. Am. Chem. Soc. 117*, 7027−7028.
28. Jordan, F., Li, H., and Brown, A. (1999) Remarkable stabilization of zwitterionic intermediates may account for a billion-fold rate acceleration by thiamin diphosphate-dependent decarboxylases, *Biochemistry 38*, 6369−6373.
29. Koland, J. G., Miller, M. J., and Gennis, R. B. (1984) Reconstitution of the membrane-bound, ubiquinone-dependent pyruvate oxidase respiratory chain of *Escherichia coli* with the cytochrome d terminal oxidase, *Biochemistry 23*, 445−453.
30. Schloss, J. V., Hixon, M. S., Chu, F., Chang, S., and Duggleby, R. G. (1996) Products formed in the oxygen-consuming reactions of acetolactate synthase and pyruvate decarboxylase, in *Biochemistry and Physiology of Thiamin Diphosphate Enzymes* (Bisswanger, H., Schellenberger, A., Eds.) pp 580−585, Intemann, Wissenschaftlicher Verlag, Prien, Germany.
31. Gruys, K. J., Datta, A., and Frey, P. A. (1989) 2-acetylthiamin pyrophosphate (acetyl-TPP) pH-rate profile for hydrolysis of acetyl-TPP and isolation of acetyl-TPP as a transient species in pyruvate dehydrogenase catalyzed reactions, *Biochemistry 28*, 9071−9080.
32. Jordan, F. (2003) Current mechanistic understanding of thiamin diphosphate-dependent enzymatic reactions, *Nat. Prod. Rep. 20*, 184−201.
33. Menon, S., and Ragsdale, S. W. (1997) Mechanism of the *Clostridium thermoaceticum* pyruvate:ferredoxin oxidoreductase: evidence for the common catalytic intermediacy of the hydroxyethylthiamine pyropyrosphate radical, *Biochemistry 36*, 8484−8494.
34. Ibdah, M., Bar-Ilan, A., Livnah, V., Schloss, J. V., Barak, Z., and Chipman, D. M. (1996) Homology modeling of the structure of bacterial acetohydroxy acid synthase and examination of the active site by site-directed mutagenesis, *Biochemistry 35*, 16282−16291.
35. Tittmann, K., Vyazmensky, M., Hübner, G., Barak, Z., and Chipman, D. M. (2004) *Proc. Natl. Acad. Sci. U.S.A.* (submitted for publication).
36. Humphrey, W., Dalke, A., and Schulten, K. (1996) VMD: visual molecular dynamics, *J. Mol. Graphics 14*, 33−38.

BI049897T